Infrared study of orientational order parameters of a ferroelectric liquid crystal

M. D. Ossowska-Chruściel,[1] R. Korlacki,[2] A. Kocot,[2,*] R. Wrzalik,[2] J. Chruściel,[1] and S. Zalewski[1]
[1]*Institute of Chemistry, University of Podlasie, 08-110 Siedlce, Poland*
[2]*Institute of Physics, University of Silesia, 40-007 Katowice, Poland*
(Received 21 January 2004; revised manuscript received 9 June 2004; published 27 October 2004)

A method of determining the set of four order parameters *S*, *D*, *P*, and *C* for a ferroelectric liquid crystal, using complementary results for different sample geometries, is presented. IR measurements have been performed for homeotropic, planar heterogeneous and, planar homogenous sample geometries. Orientational order parameters were determined in two frames of reference to obtain complete information on molecular arrangement. Results for the *D*, *P*, and *C* parameters indicate the importance of both the *intrinsic* and *extrinsic* biaxialities. The molecular rotation around the long molecular axis is not free, and the carbonyl dipole and plane of the central phenyl ring are oriented close to the tilt plane. It has been found that transition dipole moments show significant correlations, antiparallel for longitudinal dipoles and parallel for transversal ones.

DOI: 10.1103/PhysRevE.70.041705 PACS number(s): 61.30.Gd, 42.70.Df, 64.70.Md, 78.30.Jw

I. INTRODUCTION

Molecular ordering in liquid crystal phases is the basic phenomenon leading to a great variety of different liquid-crystal (LC) structures. Presently a great deal of effort is being put into elucidating the structure and polar properties of ferroelectric liquid crystals, due to their possible technological applications. Although many different theoretical models have been suggested, the microscopic origin of the organization of molecules in the chiral phases is still puzzling. A number of methods have recently been used to study the structure and orientational order of various phases [1–3].

Most applications of liquid crystals are based on using the anisotropic properties and their dependence on the pressure, temperature, and external field. Basically, the macroscopic anisotropic properties of liquid crystals are governed by their molecular behavior and the alignment and orientational order of the constituent molecules. One of the interesting problems in liquid crystals that remains to be solved is determination of the relationship between the molecular and macroscopic properties. It is therefore relevant that the various order parameters of a given liquid crystal in different phases should be determined. Any anisotropic property (electric permittivity, refractive index, magnetic susceptibility, elastic modulus, viscosity, etc.) is determined if the order parameters and corresponding molecular property are known.

Infrared spectroscopy has been found to be very useful in obtaining orientational information about molecular groups and particularly microscopic examination of the rotational motion of the dipoles around the long molecular axis [4–13]. Polarized Fourier transform infrared (FT-IR) spectroscopy can be used to study the orientational distribution and rotation of selected transition dipoles in antiferroelectric, ferroelectric, and paraelectric phases of homogeneously oriented liquid-crystal samples.

The ferroelectric liquid crystal (FLC) used in this study is a novel material with the cholesteric-chiral-smectic-*C* (Ch-Sm-*C**) phase transition sequence required for application in the half -V-shape switching mode (HV-FLC). Such a mode has been proposed in order to satisfy all conditions realizing a fast response, gray-scale control, and small spontaneous polarization, which are necessary for application in active matrix liquid-crystal displays (AM-LCD's).

In the present paper a complete set of order parameters has been obtained using IR absorbance components measured for homeotropic, planar heterogeneous, and planar homogenous sample geometries. The significance of all biaxial *D*, *P*, and *C* parameters is shown.

II. IR ABSORBANCE COMPONENTS OF THE ORDERED SYSTEMS

In an orientationally ordered material, absorbance components become dependent on the angle between the alignment axis and the polarization direction of the incident light. At a microscopic level, the infrared absorption depends on the angle between the molecular transition dipole moment μ_i, for the particular absorption band, and direction of the electrical vector of the incident light.

Using the general results for transformation of second-rank tensor properties [14], these absorbance components can be expressed in terms of transition dipole moments and orientational order parameters. If the phase is uniaxial and the effect of molecular interaction and local field can be ignored, then parallel and perpendicular components with respect to the optical axis become

$$A_{\parallel} = A_0 + B\left\{\tfrac{2}{3}S\left[(\mu_i)_n^2 - \tfrac{1}{2}((\mu_i)_l^2 + (\mu_i)_m^2)\right] + \tfrac{1}{3}D((\mu_i)_l^2 - (\mu_i)_m^2)\right\},$$

$$A_{\perp} = A_0 - B\left\{\tfrac{1}{3}S\left[(\mu_i)_n^2 - \tfrac{1}{2}((\mu_i)_l^2 + (\mu_i)_m^2)\right] + \tfrac{1}{6}D((\mu_i)_l^2 - (\mu_i)_m^2)\right\}, \quad (1)$$

where $A_0 = 1/3(A_{\parallel} + 2A_{\perp})$ is the mean absorbance of the isotropic fluid, μ_l, μ_m, and μ_n are components of the transition moment for the particular absorption, and *B* contains some fundamental constants.

*Corresponding author. Email address: kocot@us.edu.pl

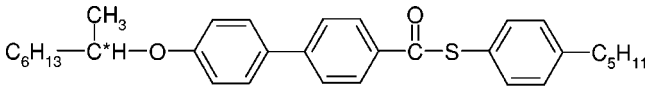

Cr 336.4 SmG* 344 SmI* 346.9 SmC* 368.1 N* 400.4 Is (heating)

Is 400.4 N* 368.1 SmC* 346.9 SmI* 344 SmG* ~ 287 Cr (cooling)

FIG. 1. Structure and phase sequence of MHOBS5. All transition temperatures are in kelvin.

If the liquid-crystalline phase is biaxial, as with tilted smectic phases, then any second-rank tensor property has three independent principal components

$$A_X = A_0 - B\left\{\tfrac{1}{3}(S-P)\left[(\mu_i)_n^2 - \tfrac{1}{2}((\mu_i)_l^2 + (\mu_i)_m^2)\right] + \tfrac{1}{6}(D-C)((\mu_i)_l^2 - (\mu_i)_m^2)\right\}, \quad (2)$$

$$A_Y = A_0 - B\left\{\tfrac{1}{3}(S+P)\left[(\mu_i)_n^2 - \tfrac{1}{2}((\mu_i)_l^2 + (\mu_i)_m^2)\right] + \tfrac{1}{3}(D+C)((\mu_i)_l^2 - (\mu_i)_m^2)\right\},$$

$$A_Z = A_0 + B\left\{\tfrac{2}{3}S\left[(\mu_i)_n^2 - \tfrac{1}{2}((\mu_i)_l^2 + (\mu_i)_m^2)\right] + \tfrac{1}{3}D((\mu_i)_l^2 - (\mu_i)_m^2)\right\}.$$

These components are expressed in terms of the general order parameters S, D, P, and C introduced for biaxial phases. They are defined by three diagonal Saupe ordering matrices, one for each of the three axes, $i=X, Y, Z$; $\alpha=x, y, z$; $S^i_{\alpha\beta} = \langle 1/2(3l_{i,\alpha}l_{i,\beta} - \delta_{\alpha\beta})\rangle$, where $l_{i,\alpha}$ is the cosine of the angle between the molecular axis α and laboratory or phase axis i.

For a uniaxial molecule the long axis ordering is described by S, while the phase biaxiality is given by $P = S^X_{zz} - S^Y_{zz}$. The molecular biaxiality in a uniaxial phase is described by the biaxial order parameter $D = S^Z_{xx} - S^Z_{yy}$, but it is possible to define a biaxial order parameter with respect to the X axis, $D' = S^X_{xx} - S^X_{yy}$, or Y axis, $D'' = S^Y_{xx} - S^Y_{yy}$. For uniaxial phases $D' = D''$ but for biaxial phases a new biaxial order parameter may be defined:

$$C = D' - D'' = (S^X_{xx} - S^X_{yy}) - (S^Y_{xx} - S^Y_{yy}).$$

It should be noted that in most cases the authors ignored the biaxial order parameters (D, P, and C) without any justification, which makes the results obtained for the S parameter rather doubtful.

III. DESCRIPTION OF THE MATERIAL

The ferroelectric LC material (S)-(+)-4-(1-methyl heptyloxy)biphenyl-(4′-pentylphenyl)-thiobenzoate (MHOBS5) was used for our experiments. The compound, from the new homologous series MHOBS*n*, where *n* denotes the number of carbon atoms in the alkyl chain, was synthesized at the Institute of Chemistry, the University of Podlasie in Siedlce (Poland). A detailed description of the synthesis, as well as the mesomorphic properties of these liquid crystals, is given elsewhere [15]. The molecular structure and phase sequence, obtained from differential scanning calorimetry (DSC) experiment, are presented in Fig. 1.

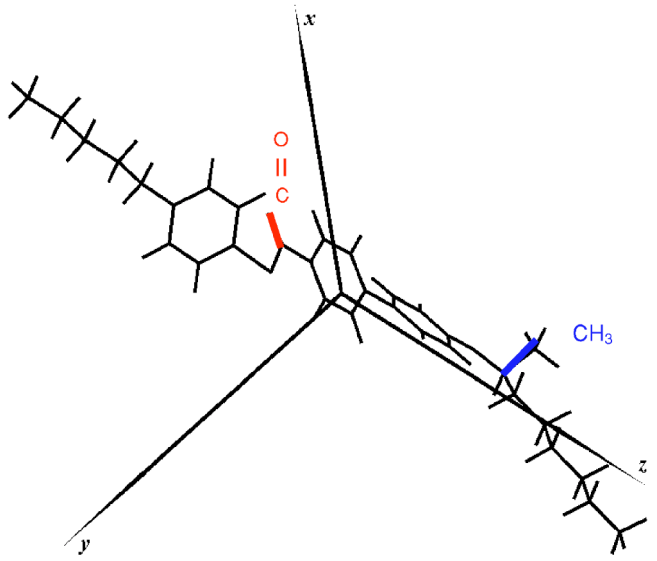

FIG. 2. (Color online) Optimized geometry and molecular frame of reference; most important groups with perpendicular dipoles have been indicated: the carbonyl group and the methyl one at chiral center.

The structure of the MHOBS5 molecule makes it very convenient for infrared examination. The structure contains only one carbonyl group (C═O), one —C—O—C group and one —C—S—C- group. Therefore, each of them can be easily identified in the experimental spectra, and used for consideration of the orientational order. To support the identification of peaks by microscopic data, the structure of the MHOBS5 molecule has been studied using the density function theory (DFT) method. Calculations were performed using the GAUSSIAN 98 application (G98W) [16] with B3-LYP functional and 6-31 polarized basis set (6-31G*). This method has already been found as very useful in obtaining the structure of complex liquid crystalline molecules [17]. Figure 2 shows the structure of the molecule and the molecular frame of reference chosen. Table I contains the most important torsion angles of the mesogen part of the molecule. Note that the central ring of the mesogen and the C—O—S group form an almost flat system and the ring planes form small angles with each other.

TABLE I. Torsion (dihedral) angles in the mesogen part of optimized geometry; all values are given with respect to the previous element of the structure specified in the table (except biphenyl); "+" indicates clockwise and "−" counterclockwise direction of the angle, looking from the chiral center of the molecule.

Groups	Torsion angles (deg)
Biphenyl	−34.9
Phenyl-carbonyl group	−2.6
COSC	−3.7
CS-phenyl	63.9

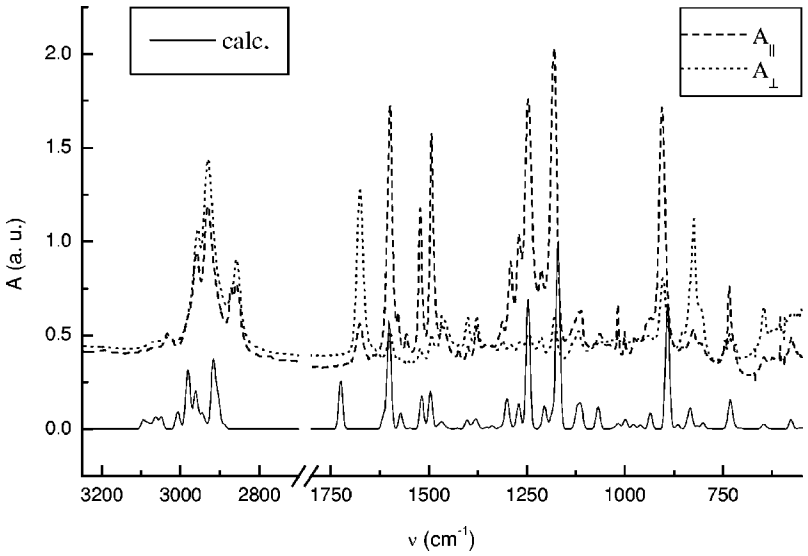

FIG. 3. Experimental and calculated IR spectra for MHOBS5: dashed line, parallel; dotted line, perpendicular components of the experimental spectra, respectively, and solid line, calculated spectra.

IV. FRAME OF REFERENCE

It is usual to choose the *z* axis of the molecular frame of reference as parallel to the long molecular axis. It is not trivial to define such an axis for the molecule with the rotational freedom of the chain segments. One of the possible methods is to choose it as the axis of the lowest moment of inertia. For the MHOBS5 molecule, this axis coincides well with the *para* axis of the biphenyl (see Fig. 2). Let us assign the *x* axis to be in plane formed by the *z* axis and the carbonyl dipole. Thus the remaining *y* axis is perpendicular to the carbonyl dipole. The dihedral angle between the carbonyl dipole and the central phenyl ring plane is about 4°, so the central phenyl ring is almost in the *z*-*x* plane of the molecular frame.

For liquid-crystal phase of uniaxial symmetry as in nonchiral nematics, for instance, the optic axis coincides with the average alignment of the molecules so that it is parallel to the director. In chiral nematics, however, the optical axis is perpendicular to the director due to the helical rotation of the director. Usually the *Z* axis is chosen along the optical axis, and since the system is uniaxial, hence the resulting absorbance components are $A_X = A_Y \neq A_Z$. If the liquid-crystal phase is biaxial as in Sm-*C* phase, then the absorbance has three independent components $A_X \neq A_Y \neq A_Z$. It is common for smectics to choose the *Z* axis of the system to be along the normal to the smectic layers.

V. EXPERIMENTAL RESULTS AND DISCUSSION

Two cells for infrared measurements were prepared using ZnSe windows and Mylar spacers: 3 μm for the homogenous and 6 μm for the homeotropic cell. Homogenous alignment was obtained by coating the windows with a polyimide film (ZLI-2650 from Merck) and rubbing in one direction. The windows were equipped with ITO (indium tin oxide) electrodes. Homeotropic orientation was forced using carboxylatochromium complex (chromolane) coatings. Both cells were filled in the cholesteric phase. The texture of the sample was observed under a polarizing microscope in order to control the quality of the alignment of the sample in a particular phase.

All infrared measurements were done with the Fourier transform infrared spectrometer Bio-Rad FTS-6000, equipped with a fast mercury cadmium telluride (MCT) detector. IR absorbance measurements were performed in the transmission mode with both orientations of the sample on cooling and on heating cycles, with a temperature step 0.5 K and accumulation over 32 scans. In the temperature range of the tilted phases, additional measurements were also done for homogenous orientation, which was obtained by applying an electric field to the planar sample. Selected peaks of the IR spectra were then fitted using a numerical approximation of the Voigt function for strong peaks and the Gaussian function for auxiliary peaks.

A. IR spectra and peak assignment

For the optimized geometry of the molecule, a vibrational spectrum has been calculated using the same settings of the DFT method as for the geometric optimization. Calculated force constants have been scaled using a scaled quantum-mechanical (SQM) procedure [18,19].

Figure 3 shows polarized vibrational IR spectra for MHOBS5 in the Sm-C^* phase and one obtained by convolution of the calculated discrete spectra with the Gaussian function of 7 cm^{-1} width. Comparison of both spectra is very helpful for assigning vibrations to selected peaks in experimental spectra. This gives us complete information on transition dipole moments μ_i, values of their components, and orientations in the molecular frame of reference. Table II shows assignment of vibrations for most important bands. Bands in the region 3100–2800 cm^{-1} do not restore well due to anharmonicity. Note that only three bands in the 1750–550 cm^{-1} region have perpendicular symmetry (1670 cm^{-1}, 825 cm^{-1}, and 650 cm^{-1}). Only the former one can be unequivocally specified.

B. Planar sample

Figure 4 shows the textures of the planar sample in various liquid-crystalline phases observed with polarized light

TABLE II. Assignment of normal modes to experimental bands.

Wave number (cm^{-1})	Assignment
2960	CH_3 asymmetric stretching
2930	CH_2 asymmetric stretching
2873	CH_3 symmetric stretching
2860	CH_2 symmetric stretching
1670	C═O stretching
1600	Phenyl ring stretching
1523	Phenyl ring stretching
1495	Phenyl ring stretching
1248	C—O—C asymmetric stretching
1180	Phenyl ring CH in plane deformation
900	Phenyl ring in plane stretching $+CH_3$ rocking
825	Phenyl ring out of plane + phenyl ring deformation $+CH_3$ scissoring
734	Phenyl ring in plane deformation $+CH_2$ scissoring
650	Phenyl ring out of plane + phenyl ring in plane deformation

and the supposed arrangements of molecules that correspond to them. Figures 5 and 6 show the absorbance behavior for planar sample of phenyl stretching (1600 cm^{-1}) and carbonyl stretching (1670 cm^{-1}), respectively.

On cooling from isotropic to nematic phase (N^*) a gradual increase of the absorbance is observed for the 1600 cm^{-1} band (Fig 5) and other bands (1495 cm^{-1}, 1180 cm^{-1}) their transition dipoles are parallel to the long molecular axis. This is due to the increase of the order of the long molecular axes in the sample plane. No IR dichroism is detectable for the planar sample in the nematic phase. Opposite behavior is observed for dipoles (650 cm^{-1}, 1670 cm^{-1}, Fig. 6), which are almost perpendicular to the long molecular axis. Small differences are noticed in the transition temperatures on the heating and cooling cycle and the level of the absorbance varies also. The alignment of the molecules was found to be planar with the helical rotation of the director; i.e., the helical axis is perpendicular to the sample plane. Such a structure is supported by the sample texture (planar or Grandjean texture) observation [see Fig. 4(a) and the structure of the phase in Fig. 4(d)]. The Z axis is usually chosen as the optical axis of the phase. The measured absorbance is therefore a perpendicular component (A_X or A_Y) for the uniaxial phase (1):

$$A_\perp/A_0 = 1 - S + \tfrac{1}{2}(3S + D\cos 2\phi)\sin^2\beta, \qquad (3)$$

where β is the angle between the transition dipole and the long molecular axis (which is the same as the z axis of the

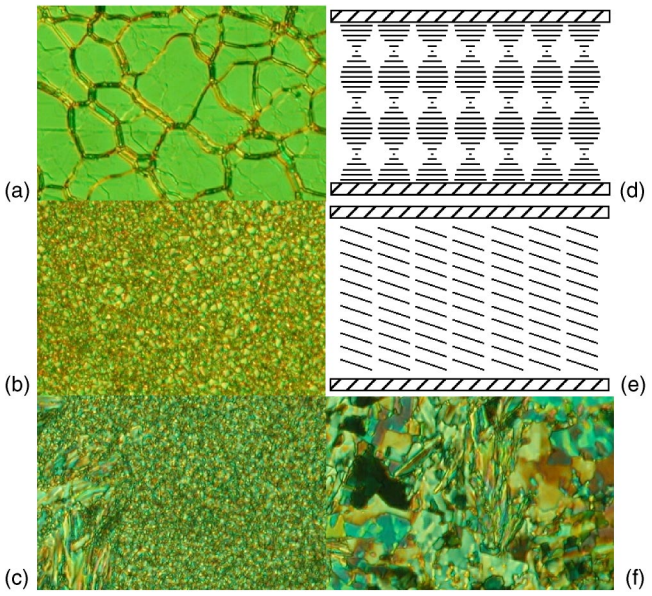

FIG. 4. (Color online) Textures of the planar sample: (a) a planar (Grandjean) texture of the cholesteric phase, (b) and (c) textures of the Sm-C^* and Sm-I^* phases, respectively, (d) and (e) arrangement of molecules in the cholesteric and smectic phases, respectively, and (f) a mosaic texture of the Sm-G^* phase.

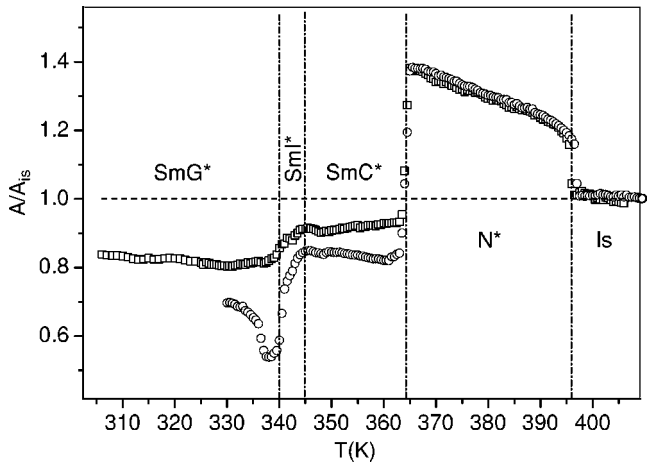

FIG. 5. Normalized absorbance of phenyl ring stretching (1600 cm^{-1}) vs temperature for the planar sample: squares, cooling cycle; circles, heating cycle.

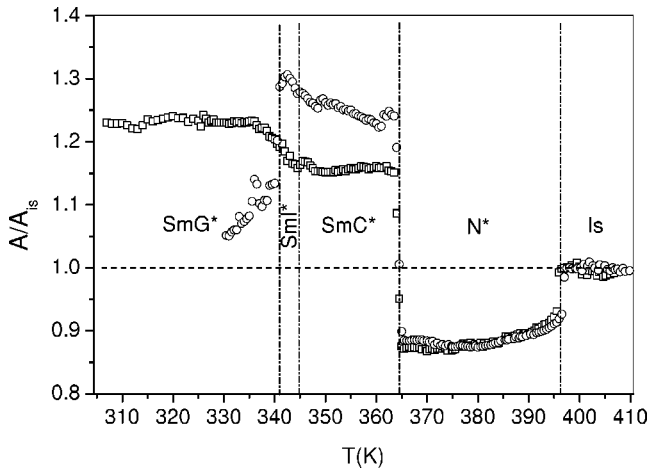

FIG. 6. Normalized absorbance of carbonyl stretching (1670 cm^{-1}) vs temperature for the planar sample: squares, cooling cycle; circles, heating cycle.

molecular frame of reference) and ϕ is the azimuthal angle between the transition dipole and x axis of the molecular system.

At the transition to Sm-C^* phase, a sudden drop of the absorbance for the parallel band (i.e., 1600 cm^{-1}) is seen primarily as a result of the structural rearrangement and, second, due to the molecular tilt. Smectic layers are arranged perpendicularly to the window plane. The helical structure is practically removed due to the small sample thickness and the director is tilted out of the cell plane, which is confirmed by optical observation. So with a polarized IR beam we can measure both the Z component of the absorbance along the optical axis and the Y component in the perpendicular direction:

$$A_Y/A_0 = 1 + (S+P)\left(\tfrac{3}{2}\sin^2\beta - 1\right) + \tfrac{1}{2}(D+C)\sin^2\beta\cos 2\phi, \tag{4a}$$

$$A_Z/A_0 = 1 + S(2 - 3\sin^2\beta) - D\sin^2\beta\cos 2\phi. \tag{4b}$$

Since the planar sample shows multidomain structure, we cannot exactly separate the Z and Y components of the absorbance. So it is more convenient to measure the planar component of absorbance, which is an average of the A_Z and A_Y components, using a nonpolarized beam.

Transitions to the Sm-I^* and further to the Sm-G^* phase are accompanied by a drop of absorbance for the parallel band and an increase for the perpendicular one. These can be partly explained by the increase of the tilt angle, but on the other hand, the increase of the orientational order may compensate it. Phase Sm-G^* is supercooled to room temperature and then the sample crystallizes. On heating the transition to the Sm-G^* phase occurs at 336 K, but other transitions are observed at temperatures similar to the ones for the cooling run.

C. Switching the planar sample by an electric field

If we apply an electric field across the sample in the Sm-C^* phase, the director rotates about 30° with respect to the alignment axis clockwise or counterclockwise depending on the sign of the field. Under a polarizing microscope this is observed as a switching the optical axis. It is useful to employ the effect to align the sample. Figure 7 illustrates one of the aligning methods possible—i.e., the transition from the cholesteric to the Sm-C^* phase under a low-voltage and high-frequency applied electric field. Due to the characteristic phase sequence (N^*–Sm-C^*) the compound exhibits the "half-V-shape switching" effect. Therefore one direction of the molecular axis is preferred [20,21]. Under sufficiently high electric field the sample shows completely unwound homogenous structure. It results in particularly high values of the IR absorbance dichroic ratio (Fig. 8). Such uniform structure was confirmed by probing azimuthal angle profile across the sample by using attenuated total reflection (ATR) IR method.

Using polarized IR spectroscopy, we can detect rotation of the absorbance profiles following application of an electric field. The advantage of this method is the ability to measure

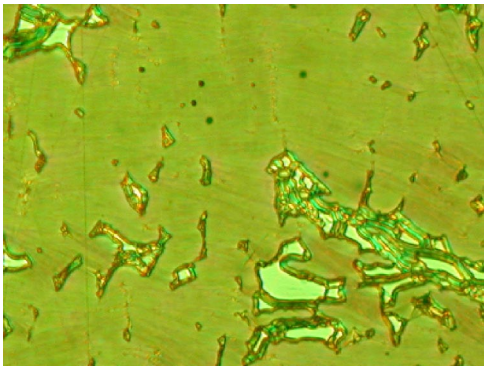

FIG. 7. (Color online) Phase transition from the cholesteric to the Sm-C^* phase with applied electric field. Remains of cholesteric phase are gradually replaced by a homogenous texture of the smectic-C^* phase.

the tilt of the transition dipoles that have different orientations in the molecular frame of reference and are located in different parts of the molecule. Figure 8 shows absorbance profiles for selected IR bands (1600 cm^{-1}, 1670 cm^{-1},

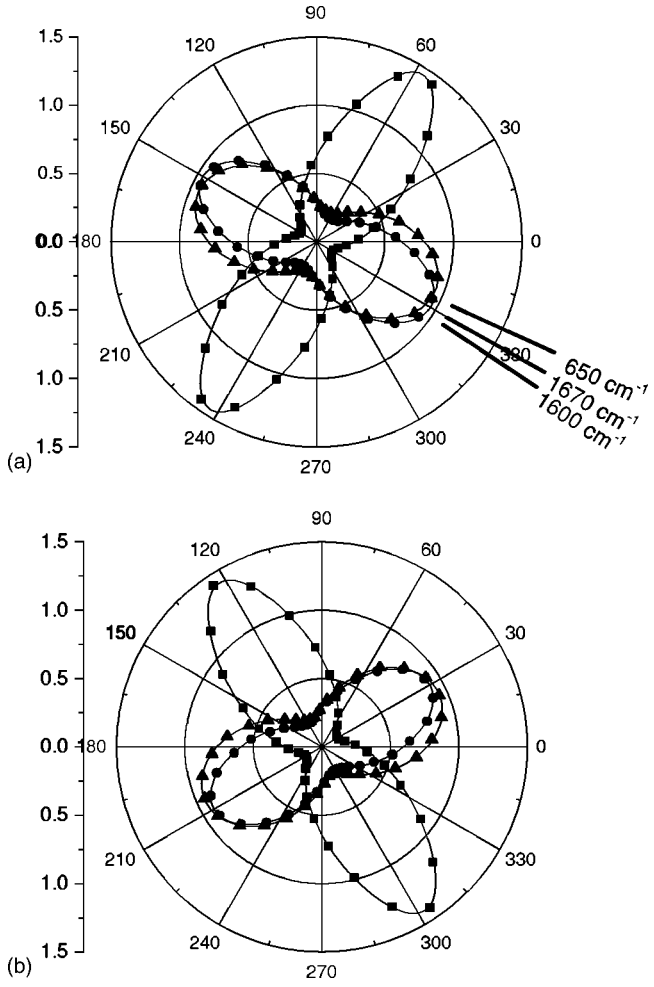

FIG. 8. Absorbance profiles vs the polarizer rotation angle in the Sm-C^* phase of the homogeneous MHOBS5 sample at 345 K: (a) for $E=-1$ V/μm, (b) for $E=1$ V/μm; squares, 1600 cm^{-1}; circles, 1670 cm^{-1}; triangles, 650 cm^{-1}; lines, fit using formula (5).

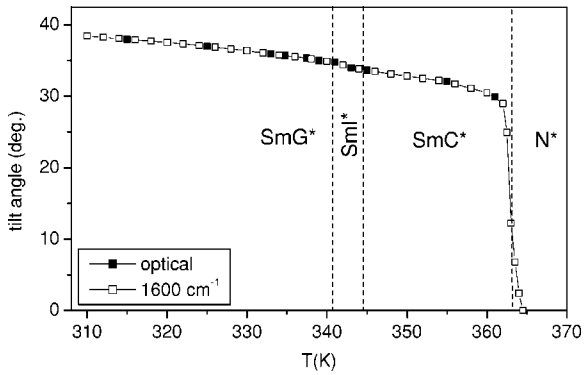

FIG. 9. Tilt angle vs temperature: solid squares, values measured optically with a polarizing microscope; open squares, values obtained from the rotation of the absorbance profile, line only for a guide to the eye.

650 cm^{-1}). The profiles are fitted using the following relation: absorbance versus polarization angle [9,10,13]:

$$A(\omega) = -\log_{10}[10^{-A_{\|}} + (10^{-A_{\perp}} - 10^{-A_{\|}})\sin^2(\omega - \omega_0)], \quad (5)$$

where $A_{\|}$ and $A_{\perp}$ are the maximal and minimal values of the absorbance, ω is the polarizer angle, and ω_0 is the angle for which a maximal absorbance is obtained. A_Z and A_X are absorbances measured at angle 0° and 90° with respect to the rubbing direction. It is clear from Fig. 8 that angles of rotation are significantly different for various IR bands under our investigation. However, the tilt angle measured for the 1600 cm^{-1} band is found to be in excellent agreement with the optical tilt angle, Fig. 9. Different tilt angles measured for various IR bands indicate the importance of the rotational biasing for spinning rotation of molecules in Sm-C^* phase [9,13].

D. Homeotropic sample

Figure 10 contains textures of the homeotropically aligned cell and the postulated molecular arrangement. Figures 11 and 12 present the absorbance dependence versus temperature of phenyl ring stretching (1600 cm^{-1}) and carbonyl stretching (1670 cm^{-1}) bands of this sample, respectively. No IR dichroism is detectable for the cell in the whole temperature range.

Absorbance in the nematic phase behaves differently. On cooling the sample shows a finger print texture [see Fig. 10(a)], while on heating a focal conic one is obtained. For the finger print texture the helical axis is in the plane of the sample film [Fig. 10(d)]; therefore, the measured absorbance is an average of the parallel and perpendicular components which in uniaxial phase can be written as

$$(A_{\|} + A_{\perp})/2A_0 = 1 + \tfrac{1}{2}S\left(1 - \tfrac{3}{2}\sin^2\beta\right) - \tfrac{1}{2}D\sin^2\beta\cos 2\phi. \quad (6)$$

In the second case, however, the helical axis is tilted with respect to the substrate plane, so the corresponding formula for the absorbance is not obvious.

In the Sm-C^* phase smectic layers are expected to be parallel to the windows of the cell. For homeotropical alignment the anchoring effect is rather weak so layered structure should not be disturbed. Therefore the absorbance in the Sm-C^* phase (like in Sm-I^* and Sm-G^* phases) is described as an average of the A_X and A_Y components:

$$(A_X + A_Y)/A_0 = 1 + S\left(\tfrac{3}{2}\sin^2\beta - 1\right) + \tfrac{1}{2}D\sin^2\beta\cos 2\phi. \quad (7)$$

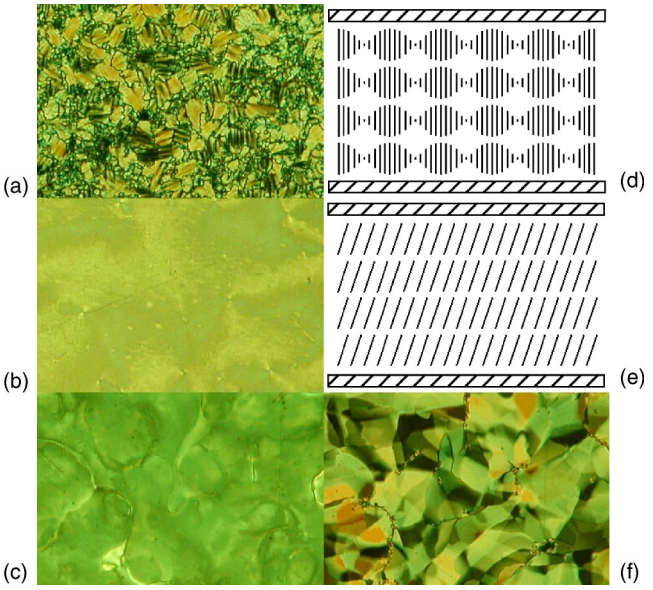

FIG. 10. (Color online) Textures of the homeotropic sample: (a) a fingerprint texture of the cholesteric phase, (b) and (c) schlieren textures of the Sm-C^* and Sm-I^* phases, respectively, (d) and (e) arrangement of molecules in the cholesteric and smectic phases, respectively, and (f) a mosaic texture of the Sm-G^* phase.

VI. CALCULATIONS OF ORDER PARAMETERS

In order to determine the order parameters let us make some simple assumptions on the molecular structure. We as-

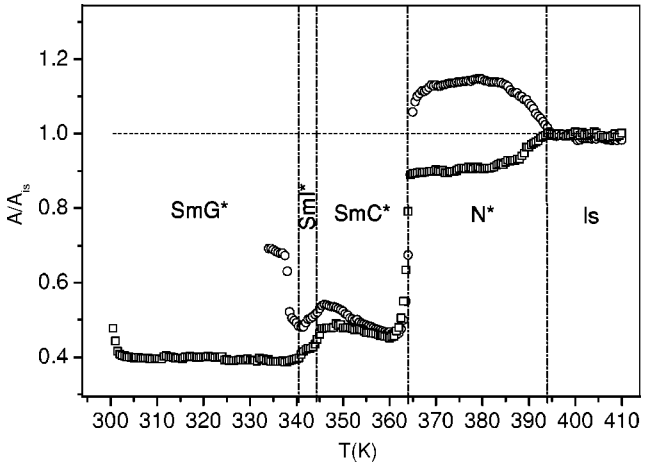

FIG. 11. Normalized absorbance of phenyl ring stretching (1600 cm^{-1}) vs temperature for the homeotropic sample: squares, cooling cycle; circles, heating cycle.

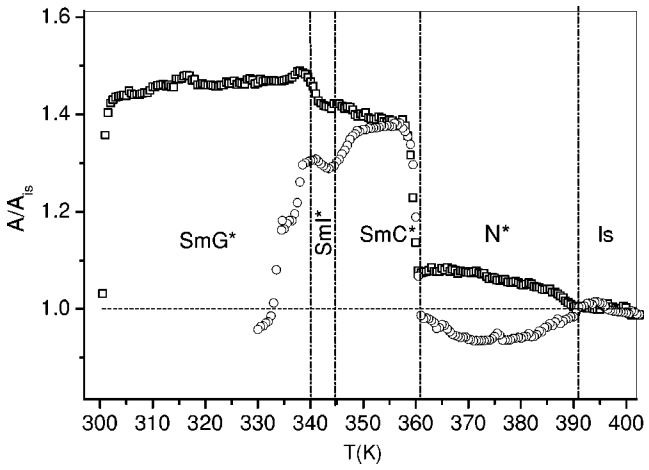

FIG. 12. Normalized absorbance of carbonyl stretching (1670 cm^{-1}) vs temperature for the homeotropic sample: squares, cooling cycle; circles, heating cycle.

sume the angles between transition dipoles and the long molecular axis is 5° for a phenyl ring (1600 cm^{-1})—this should be the mean value for three rings, unseparable in spectra—and 64° for carbonyl group stretching vibrations. Such values have been obtained from DFT calculations (see Sec. III), but they are close to the ones reported for similar ferroelectric compounds [22].

A. Correlations between transition dipole moments.

From Eqs. (2) it arises that the mean absorbance $A_0=(A_X+A_Y+A_Z)/3$ is a constant. However, if intermolecular interactions become important in the mesophase, the mean absorbance may depart from its value in the isotropic phase. Figure 13 shows the mean absorbance versus temperature, $A_0=(A_X+A_Y+A_Z)/3$. For smectic phases, the values A_X and A_Z have been taken from the measurement of the planar homogenous cell. The value A_Y has been obtained from the homeotropically aligned cell using the same values A_X and A_Y as well as the tilt angle.

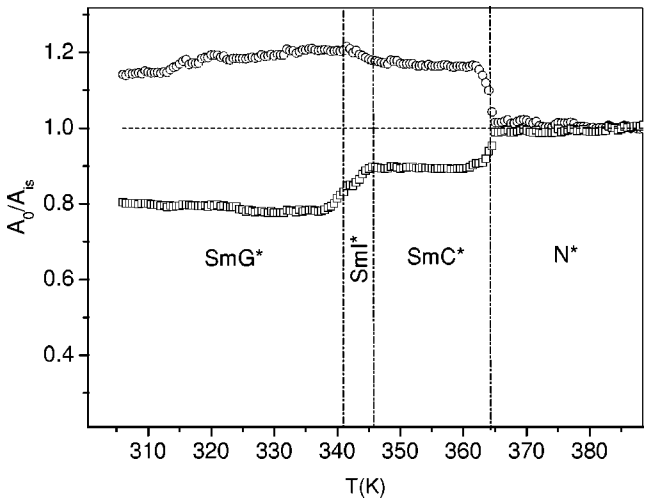

FIG. 13. Normalized mean absorbance vs temperature: squares, phenyl ring stretching (1600 cm^{-1}); circles, carbonyl stretching (1670 cm^{-1}).

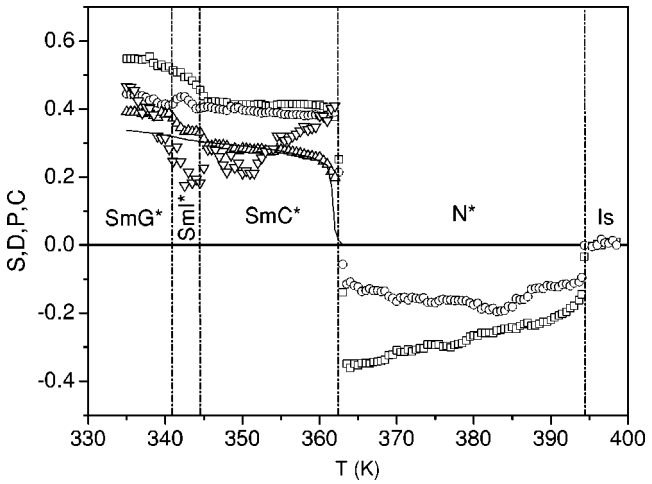

FIG. 14. Order parameters, laboratory frame: squares, S; circles, D; up triangles, P; down triangles, C; solid line, $\sin^2\theta$.

In the nematic phase the mean absorbance remains nearly the same as in isotropic phase. In the smectic phases however, we can observe a significant departure from that value which probably originated from correlations between transition dipoles. It has been found in tilted phases that longitudinal transition dipoles show preferable antiparallel orientations, but transversal dipoles have rather parallel ones due to the arrangement of the molecules in smectic layers. This effect has already been observed for permanent dipoles using dielectric spectroscopy [23]. Since the value A_0 is not constant on the transition to lower phases, it is reasonable to scale the absorbance components with respect to the average absorbance for each temperature.

B. *S*, *D*, *P*, and *C* parameters: Laboratory frame

In the nematic phase only the S and D order parameters have nonzero values. Using two chosen vibrations (1600 cm^{-1}, 1670 cm^{-1}) we can use measured values of absorbance of the planar sample and solve the two equations (3) derived for two selected bands with two variables for each temperature point. Figure 14 shows the negative value of the S order parameter approaching -0.4 at the transition to smectic phase. This indicates a good helical nematic order with helical axis perpendicular to the windows of the cell. The perfect helical-planar alignment should correspond the value $S=-0.5$. The D parameter, which indicates the molecular biaxiality, is also negative, which means that on the average the molecular y axis forms a smaller angle than the x axis with respect to the Z axis (helical axis).

For calculation of the parameters in tilted smectic phases we need to consider three independent space components of the absorbance measured for two chosen vibrations (1600 cm^{-1}, 1670 cm^{-1}). The values A_X and A_Z are measured for the planar homogenous cell. The remaining A_Y component is obtained from the homeotropically aligned cell. The results are shown in Fig. 14. The S order parameter shows a positive but rather low value, higher than 0.4. This is due to

the tilt of the molecules within the layers and such a fact is clearly indicated by parameter P. For our system of reference, P should approximately behave as a square of the tilt angle $P \cong \langle \sin^2 \theta \rangle$ [24], where θ is the tilt angle of molecules with respect to the layer normal. The solid line in Fig. 14 shows $\sin^2 \theta$, which is in perfect agreement with the P parameter in the range of the Sm-C^* phase. The differences observed in the range of low-temperature smectic phases occur since the helical structure was probably not completely unwound and hence the experimental tilt was underestimated. Reasonably the high value of D indicates the important contribution of molecular biaxiality to the IR absorbance. A positive value of D means that the molecular x axis is more tilted on the average than y axis with respect to the Z axis of the laboratory system. When we relate it to the molecular structure, it means that both the carbonyl dipole and central phenyl plane are oriented close to the molecule tilt plane.

C. *S*, *D*, *P*, and *C* parameters: Local frame

Normally, one would expect an increase of the orientational order strength with a decrease in the temperature as the amplitude of the director fluctuations becomes smaller. In tiled smectics, however, an increase of the tilt gives the opposite effect on the orientational order parameter. To be able to consider only the first effect it is convenient to introduce a local frame of reference, which is fixed with the position of the director in the particular phase. The Z axis of the system lies along the director, the Y axis is chosen perpendicular to the tilt plane of the director, and the X' is perpendicular to Z'-Y' plane, which may not be normal to the window plane of the cell.

For the planar sample in the uniaxial phase, the measured absorbance is an average of the local $A_{Z'}$ and $A_{X'}$ components [see Fig. 4(d)]. For the same sample in the smectic phases the absorbance along the alignment axis is a sum of projections of the $A_{Z'}$, and $A_{X'}$ absorbances $[A_{Z'} \cos^2(\theta) + A_{X'} \sin^2(\theta)]$. Therefore, the measured planar component is as
follows:

$$\frac{1}{2}(A_{Z'} \cos^2(\theta) + A_{X'} \sin^2(\theta) + A_{Y'}). \tag{8}$$

Following the application of an electric field, a homogenous alignment can be obtained, with molecules tilted in the window plane of the cell. So both $A_{Z'}$ and $A_{X'}$ absorbance components can be identified with directly measured $A_{\|}$ and $A_{\perp}$, respectively.

For the homeotropic sample, the helical axis of the chiral nematic phase is in the substrate plane. The absorbance component parallel to this axis is $A_{X'}$ and perpendicular is an average of $A_{Z'}$ and $A_{Y'}$ ($A_{X'}=A_{Y'}$). Therefore the measured nonpolarized absorbance can be written [see Fig. 10(d)]

$$\frac{1}{4}A_{Z'} + \frac{3}{4}A_{X'}. \tag{9}$$

In the Sm-C^* phase smectic layers are expected to be parallel to the substrates. The director is tilted in the Z-X plane; therefore, the absorbance in the Sm-C^* phase (and likely in the Sm-I^* and Sm-G^* phases) is described as follows:

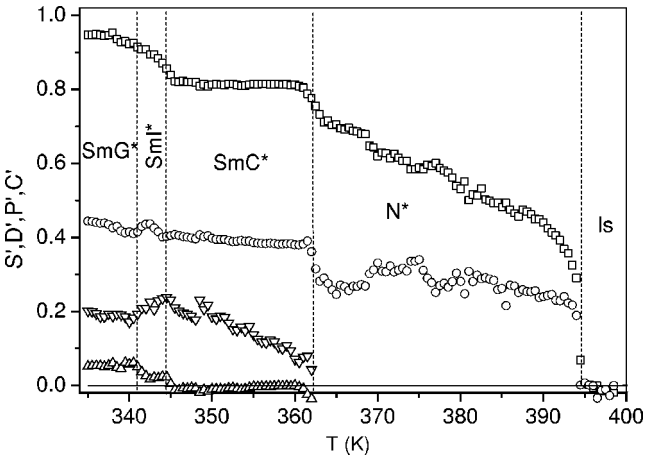

FIG. 15. Order parameters, local frame of reference: squares, S; circles, D; up triangles, P; down triangles, C.

$$\frac{1}{2}[A_{Z'} \sin^2(\theta) + A_{X'} \cos^2(\theta) + A_{Y'}]. \tag{10}$$

The absorbance components $A_{X'}$, $A_{Y'}$, and $A_{Z'}$ used above are now described by new order parameters S', D' , P', and C' defined in local frame of reference. In the nematic phase we choose a sample of planar geometry, but in smectic phases both of homogenous and homeotropic geometries for calculation of order parameters. The calculation consists of two steps: calculation the of S' and D' parameters from a sum of $A_{X'}$ and $A_{Y'}$ values (this sum depends only on S' and D'). The P' and C' parameters can be calculated from $A_{Y'}$ using previously obtained S' and D' values.

The temperature dependence of the order parameters is shown for the whole temperature range in the Fig. 15. The main order parameter S' increases monotonically, as the director fluctuations decrease during cooling. The parameter P' becomes 0 in the local system by definition, because the system is equally tilted with the director. The parameter D' provides information about biasing of the carbonyl dipole. A gradual increase (from 0.2 to 0.45) of this parameter is a measure of the biasing strength.

D. Using the order parameters to reproduce the absorbances of the planar sample

We have calculated the order parameters using experimental data of two sample geometries: homeotropic and planar homogenous. As was previously suggested, the planar sample has a *quasibookshelf* structure with the director tilted in plane perpendicular to the substrate. Now we can check this hypothesis, trying to restore absorbance values for the planar heterogenous sample in smectic phases and compare it with the experimental ones using Eqs. (2) and (8) (Fig. 16).

The agreement for the 1600-cm^{-1} band in the Sm-C^* phase is almost ideal but for the Sm-I^* and Sm-G^* slightly worse. As suggested above this may be a result of underes-

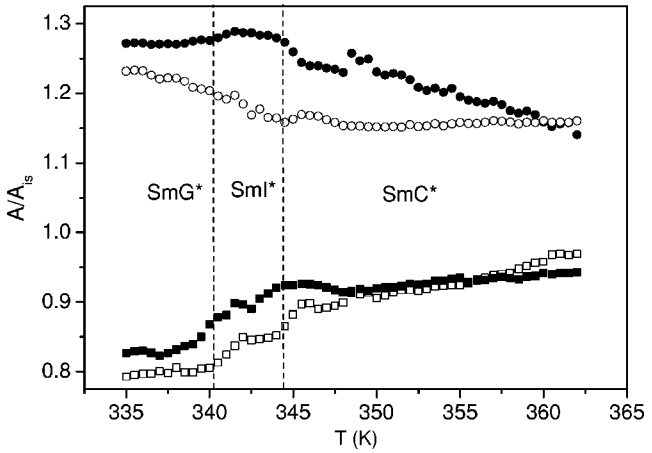

FIG. 16. Normalized absorbance vs temperature; squares, phenyl ring stretching (1600 cm^{-1}); circles, carbonyl stretching (1670 cm^{-1}); solid symbols, experimental values; open symbols, reproduced values.

timating the tilt angle values in the hexatic phases. The reproduction of the carbonyl dipole (and any perpendicular dipole) may be caused by the accuracy of assumed molecular conformation. However, the qualitative shape of both curves is satisfactory. Although the planar sample shows heterogenous alignment in smectic phases [Figs. 4(b)–4(f)], we are still able to reproduce its absorbance. In the similar way, having the set of order parameters, we can simulate any macroscopic anisotropy, if only the corresponding molecular property is known.

VII. CONCLUSIONS

The complete set of order parameters of second rank was determined in the laboratory frame of reference. In the cholesteric phase the helical-planar arrangement of the molecules is present. In smectic phases the molecules are tilted out of the substrate plane. Next, the local order was analyzed in the reference system fixed to the director. The orientational order parameter S' increases monotonically on cooling and finally approaches a reasonably high value of 0.95 in the hexatic Sm-G^* phase. The molecular biaxiality parameters, D' and C' are the measure of rotational biaxiality. Positive values indicate that both the carbonyl dipole and the central phenyl plane are oriented close to the tilt plane and that long axis fluctuations out of the tilt plane are stronger than those in the tilt plane. It is interesting to note that the molecular *intrinsic* biaxiality D', has a significant value in the nematic phase, too. It has been found in the smectic phases that longitudinal transition dipoles show antiparallel correlation, but transversal dipoles have parallel correlations due to the arrangement of the molecules in the smectic layers, as was usually observed for permanent dipoles.

ACKNOWLEDGMENTS

The authors would like to thanks Professor P. Pulay for his program for the SQM calculations, Professor A. Fukuda for useful discussions, and E. Mulry for help. We also acknowledge the financial support of the Committee for Scientific Research (KBN): Grant No. 2P03B 07025.

[1] S. T. Lagerwall, *Ferroelectric and Antiferroelectric Liquid Crystals* (Wiley, New York, 1999).
[2] J. W. Goodby, R. Blinc, N. A. Clark, S. T. Lagerwall, M. A. Osipov, S. A. Pikin, T. Sakurai, K. Yoshino, and B. Zeks, *Ferroelectric Liquid Crystals—Principles, Properties and Applications* (Gordon and Breach, New York, 1991).
[3] (a) A. Kocot, J. K. Vij, and T. S. Perova, Adv. Chem. Phys. **113**, 203 (2000);(b) Y. P. Panarin and J. K. Vij, *ibid.* **113**, 271 (2000).
[4] A. Kocot, G. Kruk, R. Wrzalik, and J. K. Vij, Liq. Cryst. **12**, 1005 (1992).
[5] E. Hild, A. Kocot, J. K. Vij, and R. Zentel, Liq. Cryst. **16**, 783 (1994).
[6] K. H. Kim, K. Ishikawa, H. Takezoe, and A. Fukuda, Phys. Rev. E **51**, 2166 (1995).
[7] K. Miyachi, J. Matsushima, Y. Takanishi, K. Ishikawa, H. Takezoe, and A. Fukuda, Phys. Rev. E **52**, R2153 (1995).
[8] F. Hide, N. A. Clark, K. Nito, A. Yasuda, and D. M. Walba, Phys. Rev. Lett. **75**, 2344 (1995).
[9] W. G. Jang, C. S. Park, J. E. Maclennan, K. H. Kim, and N. A. Clark, Ferroelectrics **180**, 213 (1996).
[10] A. Kocot, R. Wrzalik, and J. K. Vij, Liq. Cryst. **21**, 147 (1996).
[11] S. V. Shilov, H. Skupin, F. Kremer, T. Wittig, and R. Zentel, Phys. Rev. Lett. **79**, 1686 (1997).
[12] A. L. Verma, B. Zhao, S. M. Jiang, J. C. Sheng, and Y. Ozaki, Phys. Rev. E **56**, 3053 (1997).
[13] A. Kocot, R. Wrzalik, B. Orgasinska, T. Perova, J. K. Vij, and H. T. Nguyen, Phys. Rev. E **59**, 551 (1999).
[14] D. Dunmur and K. Toriyama, in *Handbook of Liquid Crystals*, edited by D. Demus, J. W. Goodby, G. W. Gray, H. W. Spiess, and V. Vill (Wiley-VCH, New York, 1998), Vol. 2A, p. 189.
[15] (a) M. D. Ossowska-Chruściel, P. Perkowski, W. Piecek, S. Zalewski, and J. Chruściel (unpublished);(b) M. D. Ossowska-Chruściel, S. Zalewski, A. Rudzki, A. Filiks, S. Głuchowski, and J. Chruściel (unpublished);(c) M. D. Ossowska-Chruściel, Liq. Cryst. **31**, 1159 (2004).
[16] M. J. Frisch *et al.*, Computer code GAUSSIAN 98 (revision A.7), Gaussian, Inc., Pittsburgh, PA, 1998.
[17] R. Wrzalik, K. Merkel, A. Kocot, and B. Cieplak, J. Chem. Phys. **117**, 4889 (2002).
[18] P. Pulay, G. Fogarasi, G. Pongor, J. E. Boggs, and A. Vargha, J. Am. Chem. Soc. **105**, 7037 (1983).
[19] G. Rauhut and P. Pulay, J. Phys. Chem. **99**, 3093 (1995).
[20] T. Hatano, K. Yamamoto, H. Takezoe, and A. Fukuda, Jpn. J. Appl. Phys., Part 1 **25**, 1762 (1986).
[21] Y. Asao, T. Togano, M. Terada, T. Moriyama, S. Nakamura, and J. Iba, Jpn. J. Appl. Phys., Part 1 **38**, 5977 (1999).

[22] J. Matsushima, Y. Takanishi, K. Ishikawa, H. Takezoe, A. Fukuda, C. S. Park, W. G. Jang, K. H. Kim, J. E. Maclennan, M. A. Glaser, N. A. Clark, and K. Takahashi, Liq. Cryst. **29**, 27 (2002).

[23] L. M. Blinov, *Electrooptical and Magnetooptical Properties of Liquid Crystals* (Wiley, New York, 1983), p. 54.

[24] K. Merkel, A. Kocot, J. K. Vij, G. Mehl, and T. Mayer, J. Chem. Phys. **121**, 5012 (2004).